Indian Journal of Fibre & Textile Research
Vol. 24, September 1999, pp. 212-218

Theoretical studies on shuttle checking: Part II—Shuttle checking by swell

P K Hari, K N Gupta, B K Behera & S G Joshi
Department of Textile Technology, Indian Institute of Technology, New Delhi 110 016, India

Received 3 February 1998; revised received and accepted 26 August 1998

Computer simulation for mathematical model of a swell has been done and the reduction in the shuttle velocity by impact with swell is predicted in terms of impactal and frictional braking. Reduction of 40% in shuttle speed by swell has been obtained and it is mainly due to impacts. The moment of inertia of swell is the most important variable and an optimum value of this parameter is required for maximum shuttle speed reduction.

Keywords: Damping ratio, Frictional checking, Impact checking, Shuttle velocity, Swell inertia

1 Introduction

In the first paper[1] of this series, theoretical equations for change in speed of shuttle and swell after impact and dynamic displacement of the swell were obtained. In this paper, analysis for shuttle braking by swell is made in terms of impact and frictional rubbing. The effect of swell inertia, damping, coefficient of restitution, shuttle mass, speed, etc. is investigated on the shuttle speed reduction by the swell system of Saurer loom shown in Fig. 1. The long pivoted swell A is also the box front. A mini swell D is located in the box back plate past the middle of the shuttle box. The picker is fixed to the picking stick and normally rests a little away from the box end. A stop C near the free end of swell limits the dynamic movement of swell. The particulars of swell, shuttle and picking stick on Saurer loom are given in Appendix-I.

2 Displacement of Swell

The displacement of swell (D_s) with respect to shuttle displacement in the box (S) at an interval of 0.01 m was measured and is shown in Fig. 2. Its equation by curve fitting is:

$$D_s = 0.6124 + 1.4165 - 0.0484\, S^2 \qquad \ldots (1)$$

This is designated as static displacement and is due to the swell profile, shuttle nose and box geometry. The angular displacement of swell (θ_S) was calculated from Eq. 1. The position of a stop which limits the movement of the swell is shown in the figure and indicates the maximum displacement of the swell D_{max} (angular displacement θ_{max}). The swell has mobility between the static curve and the stop in the region OA. Here, the impact between shuttle and swell or swell and stop is possible and the shuttle speed reduction is due to the impact with the swell. At A and beyond, the swell is in contact with the shuttle and gives frictional reduction in shuttle speed up to M. A line contact exists between swell and extreme position of the shuttle nose and thereafter due to the swell geometry the contact shifts to shuttle side wall and becomes surface contact. Frictional rubbing between swell, shuttle and box wall takes place in this region. The mini swell located at N is a light weight floating swell held in position by a spring. The mini swell after initial impact from shuttle realigns and stays in contact with shuttle. The picker/picking stick position is shown at P. The change in speed of the shuttle up to just before impact with picker was calculated in the present paper.

3 Impact Checking

The shuttle at its nose makes an initial impact with stationary swell. The velocity of shuttle and swell

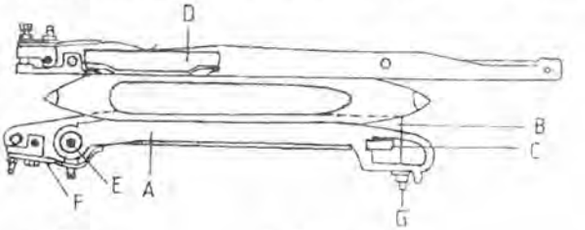

A - Swell
B - Base of box
C - Stop
D - Mini swell
E - Fulcrum
F - Spring blades
G - Stop rod finger

Fig. 1—Actual swell mechanism of Saurer loom

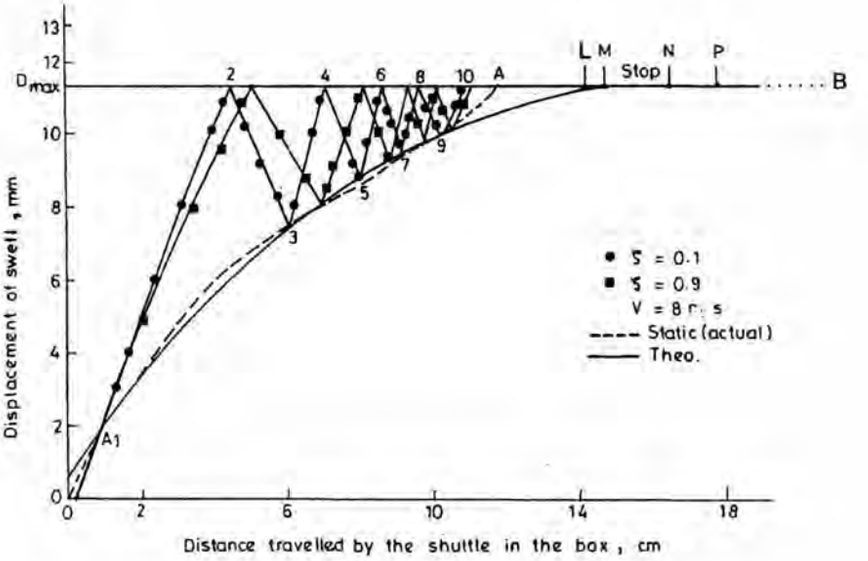

Fig. 2—Static and dynamic displacement of swell.

after impact and the dynamic displacement of swell, obtained in earlier work[1], are given by:

$$V_2 \sin\alpha = \frac{(mr_1^2 - I_1 e_1 \cos\alpha) V_1 \sin\alpha}{(mr_1^2 + I_1 \cos\alpha)}$$

$$V_2 = \sqrt{[(V_2 \sin\alpha)^2 + (V_1 \cos\alpha)^2]} \quad \ldots (2)$$

$$\omega_2 = \frac{(1+e_1)\, mr_1\, V_1 \sin\alpha \cos\alpha}{(mr_1^2 + I_1 \cos\alpha)} \quad \ldots (3)$$

For overdamped case:

$$\theta(t) = \frac{e^{-\zeta_1 \omega_n t}\, \theta(t) [e^{\omega_d t} - e^{-\omega_n t}]}{2\omega_d} - \frac{F_{PC}(l_1 + l_2)}{2(K_1 l_1^2 + K_2 l_2^2)} \quad \ldots (4)$$

For underdamped case:

$$\theta(t) = \frac{e^{-\zeta_1 \omega_n t}\, \theta(t) \sin\omega_d t}{\omega_d} - \frac{F_{PC}(l_1 + l_2)}{2(K_1 l_1^2 + K_2 l_2^2)} \quad \ldots (5)$$

where V_1 and V_2 are the shuttle velocities before and after impact; ω_2, the swell velocity after impact; and $\theta(t)$ and $\dot{\theta}(t)$, the angular displacement and velocity of the swell. In this case $\dot{\theta}(t) = \dot{\theta}(0)$ for impact with stationary swell and other variables have their usual meanings.

A break of contact between shuttle and swell takes place when the dynamic displacement of swell exceeds the static and when it equals D_{max}, another impact of swell with stop takes place. Differentiation of Eq. (4) or (5) with respect to time t gives the angular velocity of the swell at any desirable time t and from this the velocity before the next impact either with stop or shuttle can be calculated. Velocity of swell after impact from stop is obtained by multiplying swell velocity before impact with the coefficient of restitution between swell and stop (assumed as 0.9). Shuttle velocity (V_2) and swell velocity (ω_2) after impact with moving swell (angular velocity ω_1), obtained in earlier work, are given by :

$$V_2 \sin\alpha = \frac{(mr_1^2 - I_1 e_1 \cos\alpha) V_1 \sin\alpha + (1+e_1) I_1 \omega_1 r_1}{(mr_1^2 + I_1 \cos\alpha)} \quad \ldots (6)$$

$$V_2 = \sqrt{[(V_2 \sin\alpha)^2 + (V_1 \cos\alpha)^2]}$$

$$\omega_2 = \frac{(1+e_1) mr_1 V_1 \sin\alpha \cos\alpha + (I_1 \cos\alpha - mr_1^2 e_1)\omega_1}{(mr_1^2 + I_1 \cos\alpha)} \quad \ldots (7)$$

The dynamic displacement of the swell after subsequent impacts will be given by Eq. (4) or (5) without the last term on the right hand side. The process of swell impacts with stop and static swell displacement (shuttle) is repeated till the point L (Fig. 2) is reached.

4 Frictional Checking

The frictional retardation of shuttle will be by contact with the main and mini swell and also due to

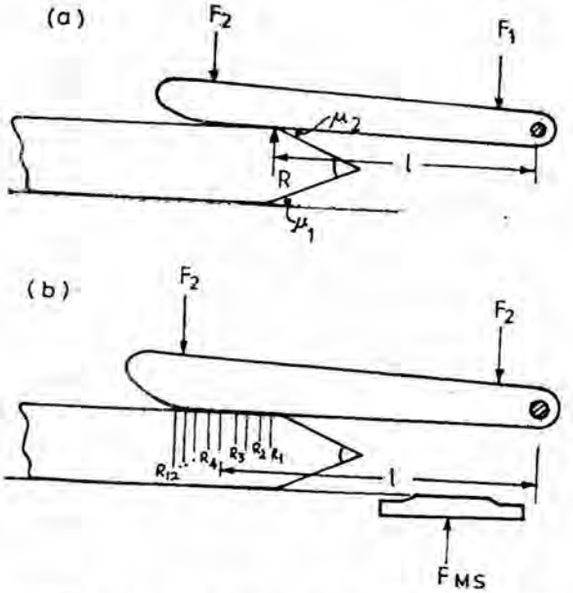

Fig. 3—Reaction force on the shuttle due to swell spring: (a) Line contact, and (b) Surface contact

the weight of the shuttle. The reaction forces on the shuttle due to the swell spring by line or surface contact are shown in Fig. 3 and their precompression are:

Line contact:

$$F' = \frac{(K_1 l_1^2 + K_2 l_2^2)\theta}{l} \text{ and } F'' = \frac{F_{PC}(l_1 + l_2)}{2l}$$

where F_{PC} is the force due to the precompression of the spring and is assumed to be equal to both springs.

Surface contact:

There would be a series of forces acting between shuttle and swell in a given contact length instead of a single reaction force

$$F' = \sum_{i=1}^{n} \frac{(K_1 l_1^2 + K_2 l_2^2)\theta}{l}$$

where n is the number of reaction forces.

Total frictional force = $(\mu_2+\mu_3)(F'+F''+F_{ms})+\mu_1 W_s$

where F_{ms} is the force on the shuttle due to mini swell and is taken equal to the product of its springs stiffness and maximum displacement; μ_1, μ_2 and μ_3, the coefficients of friction between shuttle/box bottom, shuttle/swell and shuttle/box side respectively; and W_s, the shuttle weight. The change in shuttle speed during frictional rubbing is given by:

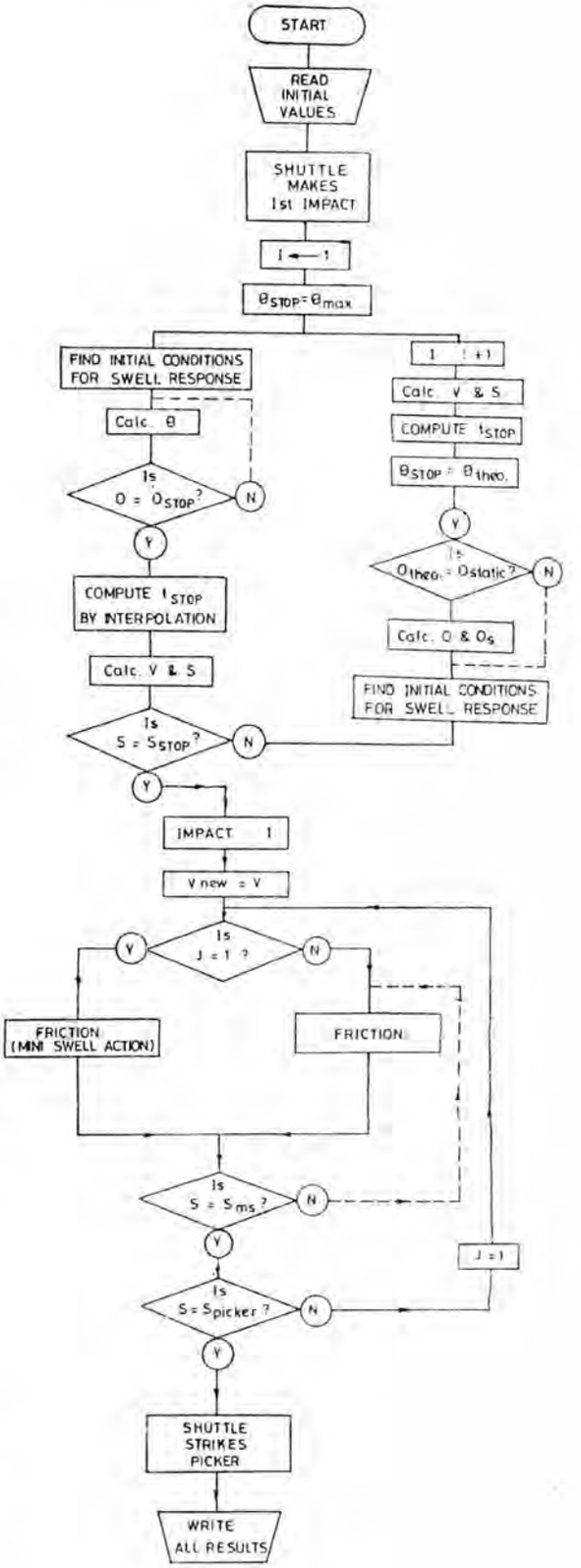

Fig. 4—Flow diagram of computer programme

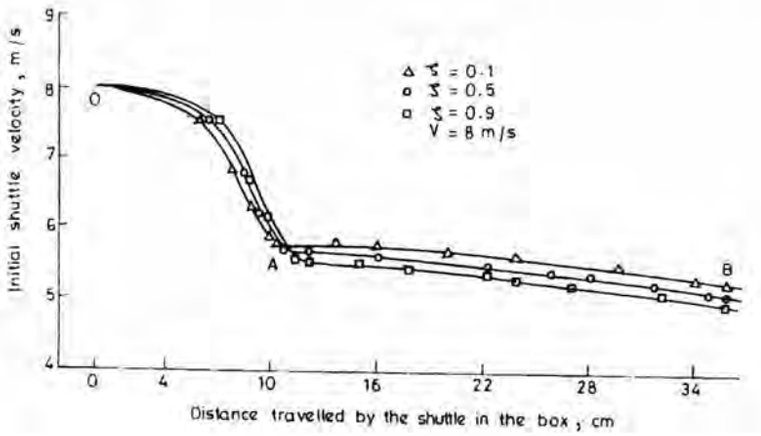

Fig. 5—Shuttle velocity reduction curve

$$\int dV = \int \left[\frac{(\mu_2 + \mu_3)(F' + F'' + F_{ms})}{m_1} + \frac{\mu_1 W_s}{m_1} \right] dt \quad \ldots \quad (8)$$

5 Computer Programming and Flowchart

A computer programme was developed for carrying the impact checking and frictional checking and iteration. The flowchart of the programme is shown in Fig. 4.

6 Results and Discussion

6.1 Dynamic Displacement of Swell

Theoretical displacement of the swell is shown in Fig. 2. The displacement of the shuttle can be divided into two regions, OA and AB. In the region OA, initially the dynamic curve (OA_1) is below the static curve. This is due to precompression of the swell springs. The swell is picking up the acceleration after receiving the impulse from the shuttle at O. When the force on the swell ($I\theta$) exceeds the forces due to swell springs, the separation between swell and shuttle takes place as shown at A_1. Then the swell makes an impact with the stop. Further swell impacts with shuttle and stop (up to 10) are shown in Fig. 2. In the regions OA_1 and AB the retardation of shuttle due to frictional rubbing with swell takes place but the retardation due to shuttle weight occurs throughout the shuttle traverse. The change in the speed of shuttle due to impacts is shown in Fig. 5. It is observed that five impacts occur between swell and shuttle but the initial shuttle impact with stationary swell gives the maximum reduction in the shuttle speed. Subsequently, shuttle impacts with moving swell give lower reduction in shuttle speed. It may be seen from Table 1 that the initial impact is not affected by changes in the initial shuttle speed or the damping ratio. However, the reduction in shuttle speed during subsequent impacts is greater for lower shuttle speed and high damping ratio. During subsequent impacts, the arm length of swell at impact will be greater for lower shuttle speed. Higher damping ratio causes more frictional dissipation of energy in the swell. These two explain lower swell angular velocity (Table 1) and thus greater reduction in shuttle speed.

Table 1—Effect of impacts on swell velocity

Shuttle velocity (V_1) m/s	ζ_1	Swell velocity[a], rad/s				
		1[b]	2[b]	3[b]	4[b]	5[b]
8	0.1	0	5.9	7.4	7.7	7.6
	0.5	0	5.2	7.3	7.3	7.2
	0.9	0	4.3	6.9	6.9	6.8
15	0.1	0	11.5	14.0	14.5	14.3
	0.5	0	10.7	13.5	14.0	13.9
	0.9	0	9.9	13.0	13.8	13.6

[a] Before impact; [b]Impact number

6.2 Shuttle Velocity Reduction by Swell

6.2.1 Effect of Damping Ratio

The swell was treated as an underdamped ($\zeta < 1$) and overdamped ($\zeta > 1$) system. The effect of damping ratio on the reduction in shuttle speed is shown in Fig. 6. An increase in damping ratio from 0.1 to 0.9 gives 3.2% and 1.7% increase in shuttle speed reduction at 8m/s and 15m/s whereas the improvement in shuttle speed reduction is 1.2% and 0.45% for an increase in damping ratio from 1.1 to 1.9. It may be no-

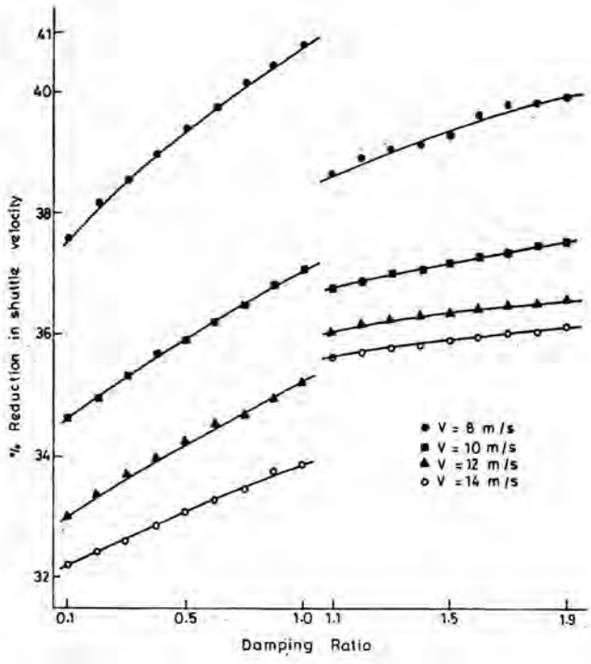

Fig. 6—Effect of damping ratio on shuttle velocity reduction

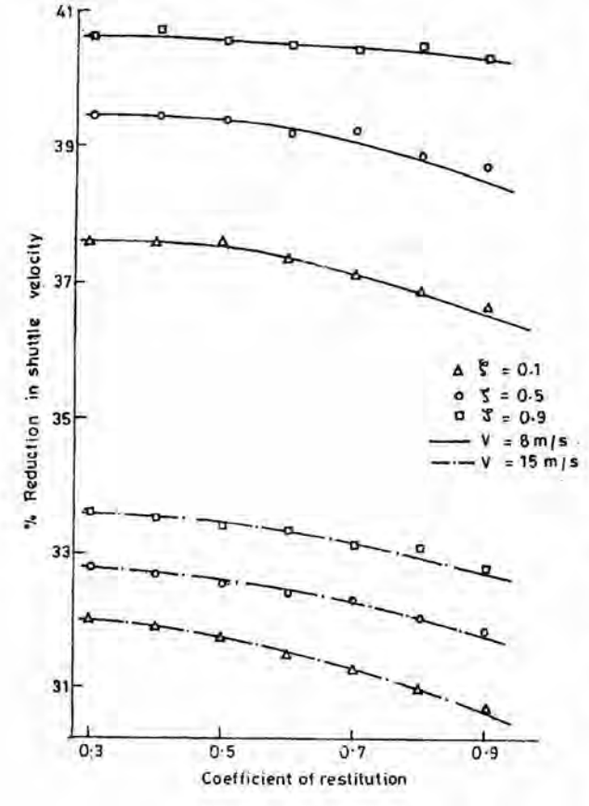

Fig. 7—Effect of coefficient of restitution between shuttle and swell on shuttle velocity reduction

Table 2—Contribution of impact and friction to shuttle braking

Shuttle velocity (V_1) m/s	% reduction in shuttle velocity due to		Total reduction in shuttle velocity %
	Impacts	Friction	
8	33.9	15.3	39.4
10	33.4	11.0	35.9
12	33.1	9.1	34.3
14	32.9	7.8	33.1

Table 3—Effect of shuttle mass on shuttle braking

Shuttle mass kg	% reduction in shuttle velocity due to		Total reduction in shuttle velocity %
	Impacts	Friction	
0.3	38.3	18.3	49.6
0.4	35.7	13.9	44.7
0.5	33.8	11.6	41.4
0.6	32.3	10.3	39.3

ticed that at higher shuttle velocity, the underdamped system is less effective towards shuttle braking.

The effect of some variables on the reduction in shuttle velocity was studied as an underdamped system ($\zeta < 1$). Fig. 5 shows the reduction in the shuttle speed by swell. It is clear that reduction in shuttle speed is much greater in the region OA, where multiple impacts between swell and shuttle took place, compared to AB where only frictional retardation to shuttle velocity was operative. This is shown in Table 2, which shows that the reduction in shuttle speed by swell is 33-39% and it is mainly due to impacts (>30%) and to a smaller extent due to the rubbing friction.

6.2.2 Effect of Initial Shuttle Speed

Table 2 shows that the reduction in shuttle speed by swell is decreased with the increase in initial shuttle velocity. This is due to reduction in the contribution by frictional braking, because the time to travel the distance AB (Fig. 1) is less. The change due to impact braking is negligible.

6.2.3 Effect of Shuttle Mass

Table 3 shows that the reduction in shuttle speed by swell is decreased with the increase in the mass of the shuttle. This reduction is due to the lower contribution by both impacts and friction. It is understandable as the increase in shuttle mass increased its momentum which will reduce the time of shuttle travel in the box.

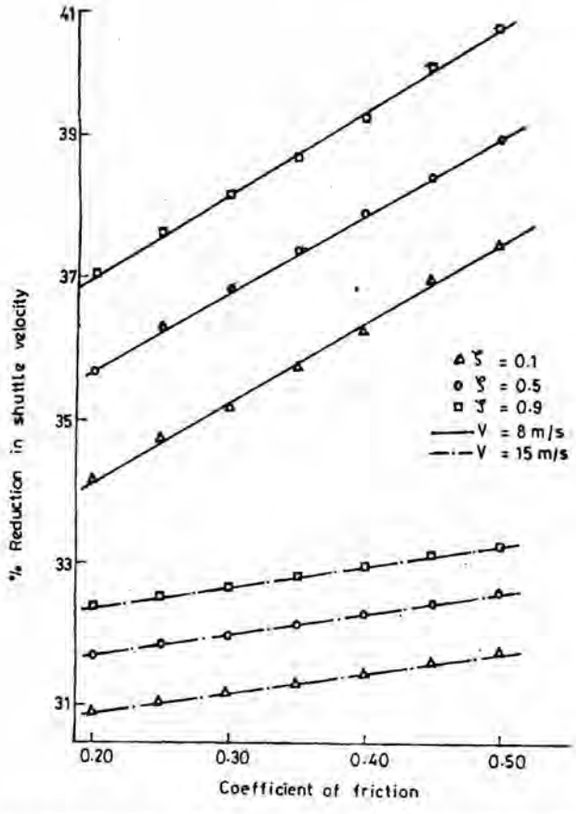

Fig. 8—Effect of coefficient of friction between shuttle and swell on shuttle velocity reduction

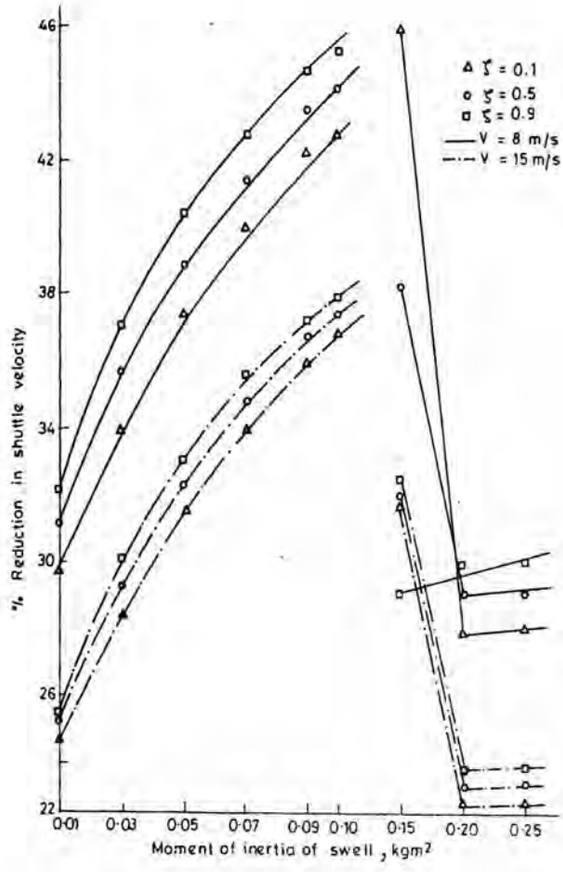

Fig. 9—Effect of moment of inertia of swell on shuttle velocity reduction

6.2.4 Effect of Coefficient of Restitution

The effect of increase in coefficient of restitution (e) between shuttle and swell on reduction in shuttle speed is shown in Fig. 7. It may be seen that variation in e does not affect the shuttle speed significantly due to lateral impacts between shuttle and swell. With 200% increase (0.3 to 0.9) in e, the reduction in shuttle speed is less than 1.5%.

6.2.5 Effect of Coefficient of Friction

Fig. 8 shows that the increase in the coefficient of friction (μ) between shuttle and swell increases the reduction in shuttle speed. An increase of 150% in μ increases the reduction in shuttle speed by only 4%.

6.2.6 Effect of Moment of Inertia of Swell

The effect of the moment of inertia of swell (I) on shuttle speed reduction is shown in Fig. 9. The reduction in shuttle speed increases sharply up to a maximum with the increase in moment of inertia of swell and then it decreases abruptly. The reduction in shuttle speed is mainly due to impacts. An increase in the moment of inertia of swell decreases the number of impacts progressively from 5 to 2. The natural frequency of the system decreases with the increase in the moment of inertia of swell and swell takes more time to return and impact with shuttle.

7 Conclusions

7.1 The maximum reduction in shuttle velocity by swell is about 40% and it is mainly due to impacts (30%).

7.2 The initial shuttle impact with stationary swell gives the maximum reduction in shuttle speed (5.5%) and subsequent impacts result in lower reduction in shuttle speed.

7.3 The moment of inertia of swell is the most important variable affecting the reduction in shuttle speed. The reduction in the shuttle speed increases to a maximum with the increase in the moment of inertia

of swell and then it decreases sharply. It is essential to decide the suitable range of the moment of inertia while designing the checking system.

7.4 Changes in the coefficient of friction and coefficient of restitution have a very little effect on the reduction in the shuttle speed by swell.

7.5 Overdamping in the swell systems is more effective for shuttle braking when high shuttle speed is used.

Reference

1 Hari P K, Gupta K N, Behera B K & Joshi S G, *Indian J Fibre Text Res,* 24 (1999) 45.

Appendix I—Particulars of swell, shuttle and picking stick on Saurer loom

I_1	=	0.526 kgm^2
K_1	=	5871 kgf/m
l_1	=	0.045 m
r_1	=	0.34 m
K_2	=	275 kgf/m
l_2	=	0.33 m
I_2	=	0.15005 kgm^2
r_2	=	0.81 m
K_3	=	570 kgf/m
α	=	20°
M	=	0.525 kg